

AN EXPERIMENTAL STUDY OF INTERFERENCE  
EFFECTS BETWEEN CLOSELY SPACED WIRES  
OF AN X-TYPE HOT-WIRE PROBE

by

FREDERICK ERNEST JEROME  
B.Sc., McMaster University, 1965

A Thesis Submitted in Partial Fulfillment  
of the Requirements for the Degree of  
Master of Science

in the Department of Physics  
and  
Institute of Oceanography

We accept this thesis as conforming to  
the required standard

September, 1971

In presenting this thesis in partial fulfilment of the requirements for an advanced degree at the University of British Columbia, I agree that the Library shall make it freely available for reference and study.

I further agree that permission for extensive copying of this thesis for scholarly purposes may be granted by the Head of my Department or by his representatives. It is understood that copying or publication of this thesis for financial gain shall not be allowed without my written permission.

Department of Physics

The University of British Columbia  
Vancouver 8, Canada

Date

Sept 15, 1971

## ABSTRACT

The Disa type 55A32 X-wire probe has been widely used in turbulence measurements. However, the author was unable to obtain agreement between turbulence measurements made simultaneously with this type of X-wire probe and an ultrasonic anemometer at the same position in the atmospheric boundary layer over the ocean. The nature of the disagreement between the two instruments suggested that there existed an unexpected response of the wires to the cross-stream wind component normal to the plane of the X-array.

Wind tunnel experiments confirmed this response and attributed most of it to thermal coupling between the two wires of the array via their hot wakes. The prongs and/or probe body were also shown to be contributors to the anomalous responses of the X-wires.

Similar experiments carried out with a Thermo-Systems model 1241-20 X-probe (with a sensor length to sensor separation ratio of 5/8 compared with 0.2 or less for the Disa 55A32 X-wire probe) demonstrated that the interference effects were absent (or, at least, insignificant).

As a consequence of these findings, the Disa Elektronik A/s company of Herlev, Denmark, modified their 55A32, 55A38 and 55A39 lines of X-wire probes to make the length/separation ratio close to unity.

## TABLE OF CONTENTS

	Page
ABSTRACT	ii
TABLE OF CONTENTS	iii
LIST OF TABLES	v
LIST OF FIGURES	vi
ACKNOWLEDGEMENTS	vii
1 INTRODUCTION	1
2 EXPECTED RESPONSE OF AN X-TYPE HOT-WIRE PROBE	2
2.1 Introduction	2
2.2 Static Characteristic for Flow Normal to Wire	2
2.3 Static Characteristic of an Inclined Wire	3
2.4 Dynamic Response of a Hot-Wire Normal to the Mean Flow	5
2.5 Dynamic Response of the Hot-Wires in an X-Array	6
3 DISCOVERY OF THE PROBLEM	10
3.1 Introduction	10
3.2 Typical Results from the Boundary Layer Experiment	12
3.3 The Disa 55A32 X-Wire Probe	14
3.4 The Intuitive Case for Thermal Wake Interference	14
3.5 Questions to be Answered	19
4 THE WIND TUNNEL EXPERIMENTS	20
4.1 Experimental Arrangement	20
4.2 Experimental Procedure	20
4.3 Experimental Results	24
4.4 Discussion of Results and Conclusions	27

	Page
4.5 The Thermo-Systems Model 1241 X-Type Hot-Film Probe	33
5 CONSEQUENCES OF THE INTERFERENCE PROBLEMS	38
5.1 - On Spectral Analysis	38
5.2 - On the Results of Other Workers	41
6 DENOUEMENT	42
BIBLIOGRAPHY	43
APPENDIX - Disa Special Information Note No. 14	45

## LIST OF TABLES

	Page
I Typical Boundary Layer Results	13
II Comparison of Calculated and Measured Spectral Estimates	41

## LIST OF FIGURES

FIGURE		Page
1.	(a) Flow Geometry for Inclined Sensor	4
	(b) Flow Geometry for X-array of Hot-Wires	4
2.	Demonstration of Linearity of Hot-Wire's Dynamic Response	7
3.	Disa 55A32 X-Wire Probe	15
4.	Orientation of 55A32 X-Probe for Field Measurements	16
5.	Experimental Arrangement in Wind Tunnel	21
6.	Block Diagram of Equipment Used to Measure Directional Characteristics of X-Probe	22
7.	v-Response of "Downstream" Wire of Disa 55A32 X-Probe	26
8.	v-Response of Disa 55A32 X-Probe	28
9.	w-Response of Disa 55A32 X-Probe	29
10.	Conventional Thermo-Systems 1241-20 Probe Used in Experiments	34
11.	v-Response of Thermo-Systems 1241-20 X-Probe	36
12.	w-Response of Thermo-Systems 1241-20 X-Probe	37

## ACKNOWLEDGEMENTS

I wish to express my appreciation to Dr. R. W. Burling for his direction during this study and to Dr. R. W. Stewart for valuable suggestions made in my discussions with him.

The Mechanical Engineering Department of the University of British Columbia kindly provided their wind tunnel for this project.

Personal financial assistance came from the National Research Council of Canada, while funds for the project were provided by the Meteorological Branch of the Canadian Department of Transport and the Defense Research Board of Canada.



## CHAPTER I. INTRODUCTION

The hot-wire anemometer has been used for many years as a research tool in fluid mechanics. It is an instrument designed for measuring rapidly changing velocities in a fluid stream through the stream's varying cooling effect on a very thin, electrically heated wire filament. The small size and rapid response of the sensing element make the hot-wire anemometer the best instrument so far developed for analysis of the velocity micro-structure of a flowing fluid. Recently the application of hot-wire anemometry has rapidly expanded due to better ancillary electronics and more interest in the details of fluid flow. Today, turbulence measurement with hot-wire anemometers is routine procedure and, with special X- or V- arrays of two independent hot-wire sensors, longitudinal and transverse components of the fluctuations in the fluid velocity can be measured simultaneously and the correlation between them can be investigated.

During the course of the analysis of turbulence data collected by the author in the atmospheric boundary layer over the ocean from hot-wire sensors in an X-configuration and from a three-dimensional ultrasonic anemometer-thermometer, it became apparent that the hot-wire sensors were not giving the expected response.

The objectives of the investigation described herein were:

- (i) to identify the problem,
- (ii) to determine the seriousness of the problem, and
- (iii) to design a sensor array that would eliminate the problem.

## CHAPTER II. EXPECTED RESPONSE OF AN X-TYPE HOT-WIRE PROBE

### 2.1 Introduction

Consider a rectangular coordinate system with the positive x-axis in the direction of the mean air flow (which will always be horizontal in these discussions). Let the z direction be vertically upward and the y direction be determined by the convention for right-handed coordinates. Then the instantaneous velocity vector can be expressed as

$$\vec{U} = \vec{i}(\bar{U} + u) + \vec{j}v + \vec{k}w \quad (2-1)$$

where  $\bar{U}$  is the mean wind speed,  $u$ ,  $v$  and  $w$  are the components of the much smaller velocity fluctuation and  $\vec{i}$ ,  $\vec{j}$  and  $\vec{k}$  are the usual unit vectors.

### 2.2 Static Characteristic for Flow Normal to Wire

A theoretical solution for the heat transfer from a uniformly heated cylinder normal to a two-dimensional, incompressible, non-viscous flow was found by King (1914). As applied to a hot-wire sensor operated in the constant temperature mode, King's Law can be expressed as

$$I^2 = A' + B'U^{1/2} \quad (2-2)$$

where  $I$  is the hot-wire current,  $A'$  and  $B'$  are constants depending on fluid and wire properties, and  $U$  is the velocity of the fluid (perpendicular to the cylinder). The idea behind the constant-temperature operation is to keep the sensing element at a constant temperature (and therefore a constant resistance) and to use the square of the heating current as the measure of the rate of cooling by heat transfer from the wire to the wind.

Since the voltage  $E$  across the wire is proportional to  $I$  in constant temperature operation, then

$$E^2 = A + BU^{\frac{1}{2}} \quad (2-3)$$

where  $A$  and  $B$  are constants. It can be seen then that the response of the hot-wire anemometer is strongly non-linear.

### 2.3 Static Characteristic of an Inclined Wire

If the flow direction is not normal to a cylindrical sensor but rather makes an angle  $\theta$  with the normal to the sensor as shown in Fig. 1a, the directional sensitivity of the hot-wire anemometer must be known. Equivalently, an "effective (normal) cooling velocity" should be obtainable from the actual mean velocity, the geometry and sensor characteristics (such as length to diameter ratio).

Normal component or "cosine law" cooling is usually assumed (Hinze, 1959; Corrsin, 1963). This means that the heat transferred from the hot-wire to the fluid flow depends only on the component of the fluid velocity normal to the wire. For the configuration in Fig. 1, the effective cooling velocity,  $C$ , would then be

$$C = \bar{U} \cos \theta.$$

Hinze (1959) and Webster (1962) have suggested what has become the most widely accepted expression for the effective cooling velocity taking into account tangential component cooling as well as normal component cooling, i.e.,

$$C^2 = \bar{U}^2 (\cos^2 \theta + k^2 \sin^2 \theta). \quad (2-4)$$

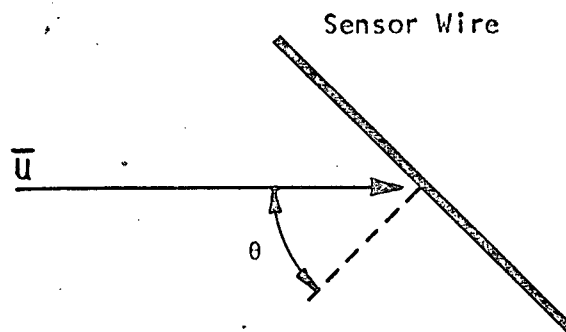


Fig. 1(a). Flow Geometry for Inclined Sensor

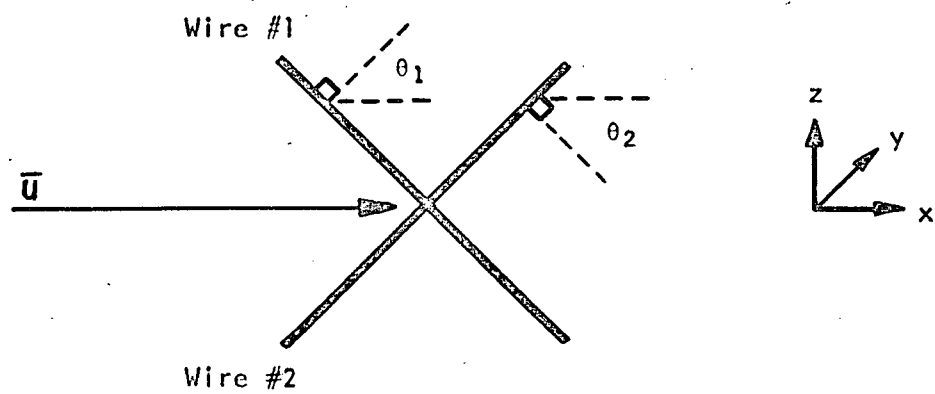


Fig. 1(b). Flow Geometry for X-array of Hot Wires

Champagne (1967) found that  $k$  depends on the parameters that govern the temperature distribution along the wire, primarily the length-to-diameter ratio ( $l/d$ ) of the wire.

For the wires used in the present study,

$$\frac{l}{d} \doteq \frac{1.0 \text{ mm.}}{0.005 \text{ mm.}} = 200$$

and Champagne determined  $k = 0.20$  for this ratio. Since  $\theta \doteq 45^\circ$  for the experiments herein, then there is only a 2% error introduced by calculating the effective cooling velocity assuming normal component cooling. This is a much smaller effect than the one being studied, so normal component cooling with its attendant mathematical simplicity will be assumed and King's Law becomes

$$E^2 = A + BC^{\frac{1}{2}}. \quad (2-5)$$

#### 2.4 Dynamic Response of a Hot-Wire Normal to the Mean Flow

Consider a hot-wire sensor aligned parallel to the  $z$ -axis in a turbulent air flow described by equation (2-1). Assuming normal component cooling,

$$\begin{aligned} C &= \{(\bar{U} + u)^2 + v^2\}^{\frac{1}{2}} \\ &= \bar{U}\{1 + 2u/\bar{U} + u^2/\bar{U}^2 + v^2/\bar{U}^2\}^{\frac{1}{2}} \\ &= \bar{U}\{1 + u/\bar{U} + u^2/(2\bar{U}^2) + v^2/(2\bar{U}^2) - u^2/(2\bar{U}^2) + \text{higher order terms}\}. \end{aligned}$$

The effective cooling velocity can be considered to consist of a mean part

$$\bar{C} = \bar{U} + \overline{v^2}/(2\bar{U}) + \text{higher order terms} \quad (2-6)$$

and a fluctuating part

$$c = u + (v^2 - \overline{v^2}) / (2\overline{U}) + \text{higher order terms.} \quad (2-7)$$

Hinze (1959) and Pond (1965) have argued that even for turbulence intensities,  $(u^2)^{1/2} / \overline{U}$ , as high as 0.1, the second and higher order terms in equation (2-6) and (2-7) and in the Taylor expansion of King's Law about  $C = \overline{C}$  can be omitted with only a 2% error. This means that for low intensity turbulence, the dynamic response,  $e$ , of a single vertical hot-wire is essentially linear, i.e.,

$$e = \frac{B}{4\overline{EC}^{1/2}} c \quad (2-8)$$

$$= \frac{B}{4\overline{EU}^{1/2}} u. \quad (2-9)$$

Figure 2 provides experimental justification for assuming a linear response for a turbulence intensity near 0.1 (in the atmospheric boundary layer over the sea). It shows  $e$  as determined by equation (2-9) plotted against  $u$  as measured simultaneously at the same position by a sonic anemometer, a linear response instrument. Each point represents a 0.8 second time average. Note that the zeros on the axes were determined using the mean wind speed (9.2 m/sec) for a period of time longer than the period represented by the data in the figure. The mean wind speed for this shorter interval was slightly greater than 9.2 m/sec resulting in the apparent skewness of the data in Fig. 2.

## 2.5 Dynamic Response of the Hot-Wires in an X-array

Fig. 1b (page 4) shows two inclined wires in an X-configuration in the xz-plane. The wires are mounted close together (but not touching) on a single probe. They are operated as two independent inclined wires.

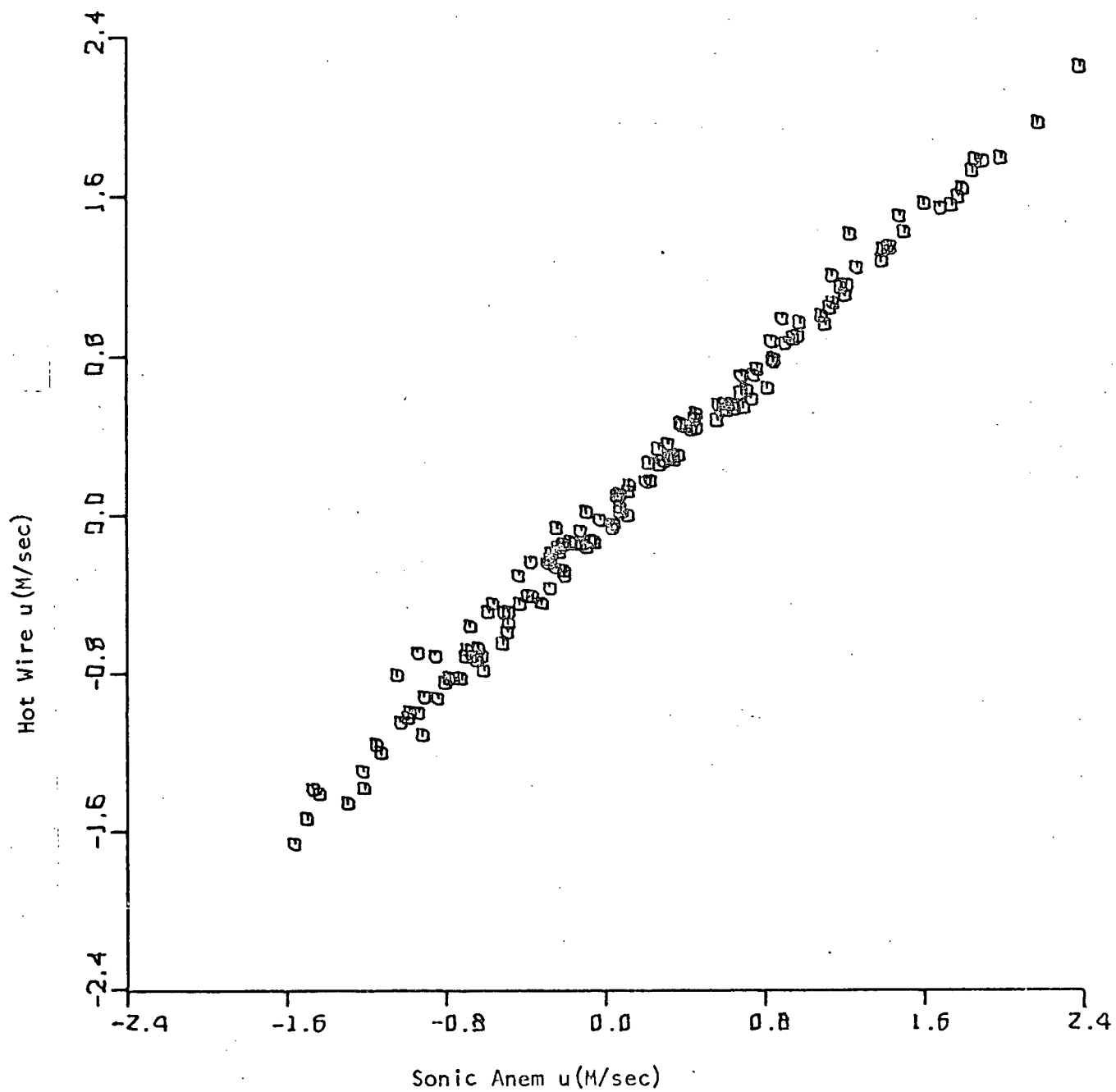


Fig. 2. Demonstration of Linearity of Hot-Wire's Dynamic Response.

For wire no. 1, the effective cooling velocity in a turbulent flow described by equation (2-1) is

$$\begin{aligned}
 C_1 &= \{(\bar{U} + u) \cos \theta_1 + w \sin \theta_1\}^2 + v^2\}^{\frac{1}{2}} \\
 &= \bar{U} \cos \theta_1 \{1 + 2u/\bar{U} + 2(w \tan \theta_1)/\bar{U} + u^2/\bar{U}^2 \\
 &\quad + 2(uw \tan \theta_1)/\bar{U}^2 + (w^2 \tan^2 \theta_1)/\bar{U}^2 \\
 &\quad + (v^2 \sec^2 \theta_1)/\bar{U}^2\}^{\frac{1}{2}} \\
 &= \bar{U} \cos \theta_1 \{1 + u/\bar{U} + (w \tan \theta_1)/\bar{U} + \text{higher order terms}\}.
 \end{aligned}$$

As in the case of the vertical wire and a turbulence intensity < 0.1, second and higher order terms can be dropped from expressions for  $\bar{C}$  and  $c$  with a resulting error in  $c$  of only about 2%. The voltage fluctuations across wire no. 1 are, to a good approximation linearly related to  $u$  and  $w$ , i.e.,

$$e_1 = \frac{B_1 (\cos \theta_1)^{\frac{1}{2}}}{4\bar{E}_1 \bar{U}^{\frac{1}{2}}} (u + w \tan \theta_1) \quad (2-10)$$

or

$$e_1 = a_1 u + b_1 w \quad (2-11)$$

where the definitions of  $a_1$  and  $b_1$  are apparent. In practice,

$\theta_1 \doteq 45^\circ$  so that  $a_1 \doteq b_1$ .

Similarly the dynamic response equation for wire no. 2 is

$$e_2 = \frac{B_2 (\cos \theta_2)^{\frac{1}{2}}}{4\bar{E}_2 \bar{U}^{\frac{1}{2}}} (u - w \tan \theta_2) \quad (2-12)$$



or

$$e_2 = a_2 u - b_2 w \quad (2-13)$$

From equations (2-11) and (2-13), it can be seen that two hot-wires in an X-array can be used to measure two components of the velocity fluctuation vector - the downstream component and the transverse component in the plane of the "X". Any response to the transverse component perpendicular to the plane of the "X" is expected to be a higher order effect.

## CHAPTER III. DISCOVERY OF THE PROBLEM

3.1 Introduction

As part of the air-sea interaction research program conducted by the Institute of Oceanography, the author intended to investigate certain features of the wind turbulence microstructure in the atmospheric boundary layer over the ocean. Instruments were mounted on a tower standing on a tidal flat. Water depth varied from 0 at low spring tide to 14 ft. at high spring tide.

The experimental plan was to use an X-array of hot-wires in conjunction with a three-dimensional ultrasonic anemometer-thermometer. It has been a long-standing practice in the air-sea interaction program to make simultaneous measurements of a micrometeorological or oceanographic quantity with two instruments using different principles of operation if possible. Often the instruments used were newly developed or were being used in an environment for which they were not designed or their calibration stability was suspect. Therefore the duplication of measurement was necessary to "keep the instruments honest" (not to mention the graduate students).

In the particular field experiment being described, the presence of the sonic anemometer had a more important purpose. Hot-wire anemometers, having a highly non-linear static characteristic (section 2.2), present considerable calibration difficulties. The

mean wind must be well known and steady for a reliable dynamic calibration (equations (2-9), (2-10) and (2-12)). As if that were not enough, their stability of calibration is suspect (Weiler, 1966) especially if contamination of the wire surface (by salt-water spray, for example) is a possibility and, in the constant temperature mode of operation, the static calibration seems to deviate from King's Law - the characteristic is better approximated by

$$E^2 = A + BU^{0.45}$$

according to Collis and Williams (1959). A further problem with X-arrays of hot-wires is to accurately reproduce in the field the probe alignment used during calibration.

The sonic anemometer (Kaijo Denki, Model PAT-311-1), on the other hand, has minimal calibration procedures - only certain electrical adjustments need to be infrequently checked - and has a linear response at the wind speeds encountered. This anemometer has been described by Mitsuta (1966). It is useful for measuring only the larger scale (and lower frequency) turbulence fluctuations, including scales which contribute to most of the atmospheric momentum and heat fluxes, because it determines the spatial average of the component of the wind velocity over each of three 20 cm. path lengths arranged in a special geometry.

The intention was to use the sonic anemometer measurements to provide an "in situ" dynamic calibration of the hot-wires. With  $u$ ,  $v$ , and  $w$  all obtainable from the sonic anemometer data, and simultaneous measurements of the hot-wire voltages  $e_1$  and  $e_2$  (equations (2-11), (2-13)) at essentially the same position, then the hot-wire dynamic calibration constants  $a_1$ ,  $b_1$ ,  $a_2$  and  $b_2$  can be calculated. Since spectral analysis

of quantities like  $\overline{u^2}$ ,  $\overline{w^2}$  and  $\overline{uw}$  - the overbar indicating a time average - were to be obtained in the end, one technique employed finding the planes of regression of  $\overline{e_1^2}$  and  $\overline{e_2^2}$  on  $\overline{u^2}$ ,  $\overline{uw}$  and  $\overline{w^2}$ . To elaborate further, from equation (2-11),

$$\overline{e_1^2} = a_1^2 \overline{u^2} + 2a_1 b_1 \overline{uw} + b_1^2 \overline{w^2} . \quad (3-1)$$

The frequency spectra of  $\overline{u^2}$ ,  $\overline{uw}$ , and  $\overline{w^2}$  from sonic anemometer data and of  $\overline{e_1^2}$  from the no. 1 hot-wire voltage signal were computed. Then using the spectral estimates from about fifteen third-octave bandwidths at low frequencies where the sonic response has not begun to fall off, a computer program calculated three constants P, Q and R for the plane of "best fit" (in the least squares sense), i.e.,

$$\overline{e_1^2} = P \overline{u^2} + Q \overline{uw} + R \overline{w^2} . \quad (3-2)$$

Then,

$$a_1 = P^{\frac{1}{2}} \text{ and } b_1 = R^{\frac{1}{2}} .$$

This technique provided a check since equation (3-1) shows that P, Q and R are not independent but rather

$$Q = 2(PR)^{\frac{1}{2}} .$$

The calibration for wire No. 2 was similarly obtained.

### 3.2 Typical Results from the Boundary Layer Experiment

Once the dynamic calibrations of the hot-wires had been worked out as described in section 3.1, a wide variety of autospectral and cospectral analyses were performed. Table I presents typical results from one data record for third-octave bandwidths about three centre

frequencies,  $f$ . A subscript h or s indicates whether the subscripted quantity was determined from hot-wire or sonic anemometer data respectively.

$f \text{ (sec)}^{-1}$	$5.19 \times 10^{-2}$	$1.16 \times 10^{-1}$	$1.77 \times 10^{-1}$
$\overline{U_s^2} \text{ (m/sec)}^2$	$8.27 \times 10^{-1}$	$3.31 \times 10^{-1}$	$2.03 \times 10^{-1}$
$\overline{U_h^2} \text{ (m/sec)}^2$	$7.54 \times 10^{-1}$	$3.03 \times 10^{-1}$	$1.81 \times 10^{-1}$
$\overline{W_s^2} \text{ (m/sec)}^2$	$4.94 \times 10^{-2}$	$3.48 \times 10^{-2}$	$3.33 \times 10^{-2}$
$\overline{W_h^2} \text{ (m/sec)}^2$	$1.41 \times 10^{-1}$	$5.34 \times 10^{-2}$	$5.19 \times 10^{-2}$
$\overline{V_s^2} \text{ (m/sec)}^2$	$4.32 \times 10^{-1}$	$1.44 \times 10^{-1}$	$9.96 \times 10^{-2}$
$\overline{U_s W_s} \text{ (m/sec)}^2$	$-1.24 \times 10^{-1}$	$-5.80 \times 10^{-2}$	$-2.84 \times 10^{-2}$
$\overline{U_h W_h} \text{ (m/sec)}^2$	$-1.06 \times 10^{-1}$	$-5.78 \times 10^{-2}$	$-2.78 \times 10^{-2}$
$\overline{V_s W_s} \text{ (m/sec)}^2$	$6.85 \times 10^{-3}$	$5.68 \times 10^{-4}$	$5.61 \times 10^{-3}$
$\overline{V_s W_h} \text{ (m/sec)}^2$	$2.04 \times 10^{-1}$	$6.18 \times 10^{-2}$	$5.13 \times 10^{-2}$

TABLE I: Typical Boundary Layer Results

The most dramatic discrepancies occur between  $\overline{w_h^2}$  and  $\overline{w_s^2}$  and between  $\overline{v_s w_h}$  and  $\overline{v_s w_s}$ . The results indicate that the quantity being called  $w_h$  was contaminated by something correlated with  $v_s$  but only weakly, if at all, correlated with  $u_s$ .

Recall from the discussion in section 2.5 that the response of the wires of an X-array (with the plane of the "X" aligned parallel to the xz-coordinate plane) to  $v$  fluctuations is expected to be negligible in low intensity turbulence. Furthermore, the shear flow in the boundary layer at the field site is expected to be essentially horizontally homogeneous. Consequently  $v$  is not expected to be strongly correlated

with  $u$ ,  $w$  or density fluctuations. This view is supported by a comparison of  $\overline{v_s w_s}$  with  $\overline{u_s w_s}$  in Table I. The latter correlation is typically an order of magnitude greater than the former. There must have been a mechanism whereby the hot-wires were directly responding to  $v$  in such a manner that the analysis procedure attributed the spurious response to a  $w$  fluctuation. In other words,  $v$  fluctuations contributed responses of similar polarity (in  $e_1$  and  $e_2$ ) to those caused by  $w$  fluctuations.

### 3.3 The Disa 55A32 X-wire Probe

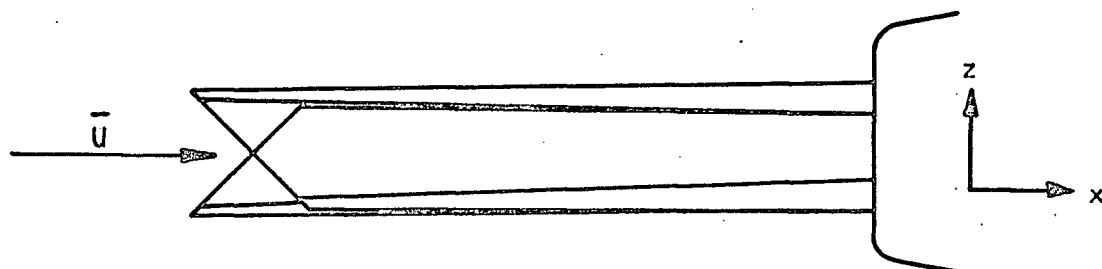
The X-wire probes used in the field experiment were Disa Elektronik (of Denmark) type 55A32. The details of the probe tip and wire arrangement are shown in Fig. 3. This type and other Disa types with similar wire lengths and wire separations have been widely used in turbulence measurements. The wires themselves are platinum-plated tungsten 5 microns in diameter.

The configuration of the wires for the field measurements described in this chapter is shown in Fig. 4.

### 3.4 The Intuitive Case for Thermal Wake Interference

The main effect of  $v$  fluctuations for

$$|v| < 0.1 \bar{U}$$



Wire lengths =  $1.00 \pm 0.05$  mm

Dia of prong tips =  $0.11 \pm 0.01$  mm

Separation of wires =  $0.16 \pm 0.01$  mm

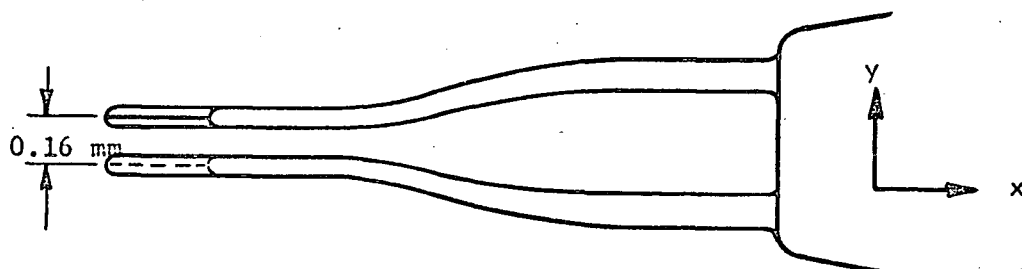


Fig. 3. Disa 55A32 X-Wire Probe

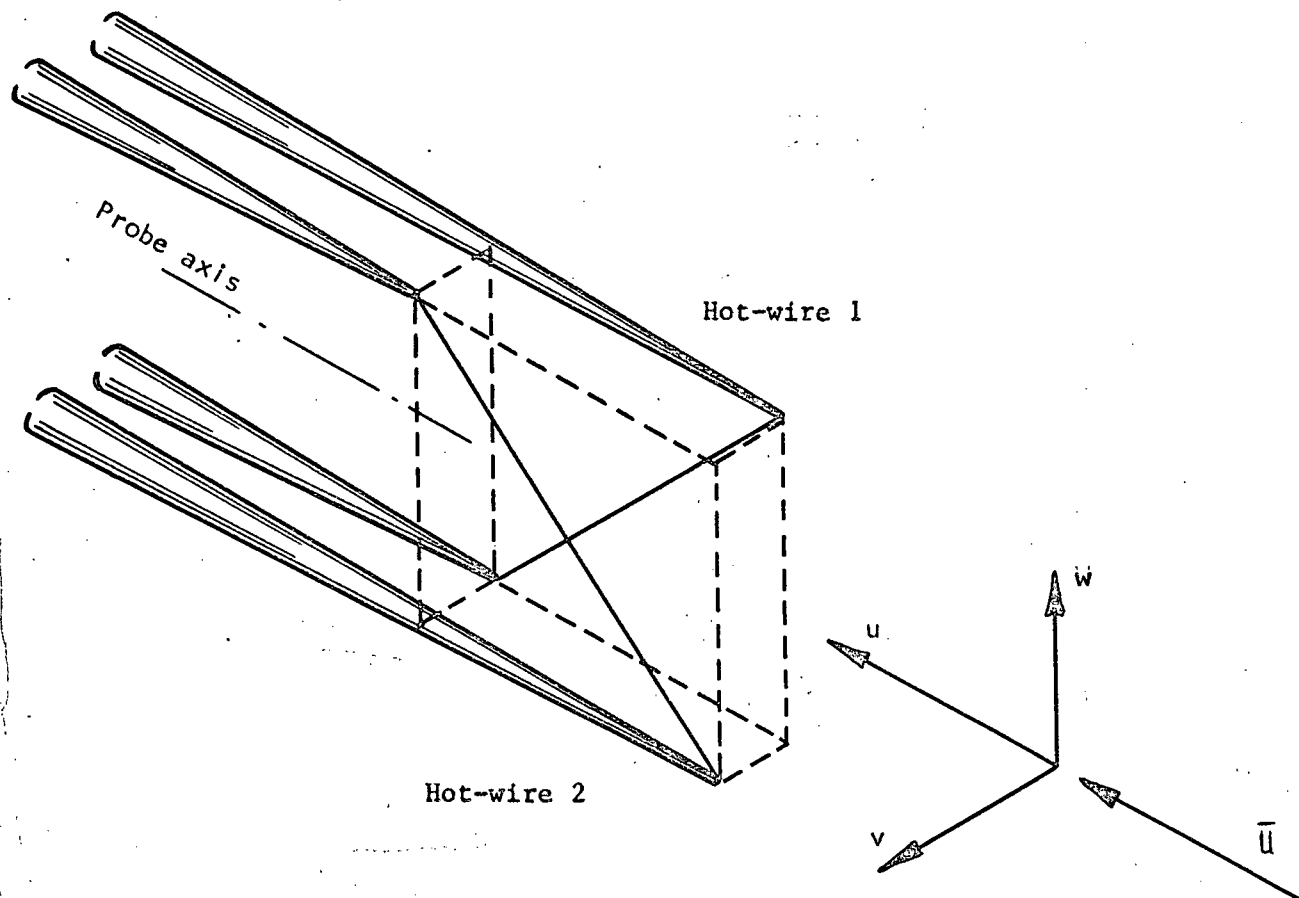


Fig. 4. Orientation of 55A32 X-probe for field measurements



is to rotate the instantaneous wind velocity vector in the horizontal plane by an angle

$$\beta = \tan^{-1}(v/\bar{U})$$

rather than to appreciably alter the length of the wind vector. For 1 mm. long wires separated by 0.16 mm. in an X-array, a wind velocity vector lying in the xy-plane but making an angle with the xz-plane of

$$\tan^{-1} \frac{0.16}{0.71} = 22.5^{\circ}$$

will cause an end of one wire to lie directly downwind of an end of the other wire (see Fig. 4 again). If the X-wire array were initially aligned properly and the mean wind direction were to remain steady, then instantaneous rotations of this size in the horizontal caused by  $v$  fluctuations would be extremely rare for a root-mean-square turbulence intensity of 0.1.

However, the wake of a wire is expected to broaden as it is convected downstream. Furthermore, the influence of the wire supporting system consisting of prongs and the probe body may further broaden the wake. Hoole and Calvert (1967), Gilmore (1967) and Norman (1967) have all investigated the directional characteristics of the Disa Type 55A25 single hot-wire probe with the wire aligned normal to an air flow. They found a 15 - 20% variation in the indicated velocity as the probe was rotated  $\pm 90^{\circ}$  about the wire axis from a position with the probe axis parallel to the flow direction. They concluded that prongs and probe body were about equally responsible for the flow displacement at the position of the wire. Eyre (1967) made similar measurements with the same type of probe and his experimental results agree well with those

reported by the above authors. However, his explanation of the cause of the directional sensitivity for rotation about the wire axis is quite different. He attributes the whole effect to an angular-dependent variation of convective heat loss from the prongs and a consequent change of heat conduction from the wire ends.

Dahm and Rasmussen (1969) studied the dependence of the directional sensitivity for rotation about the wire axis on prong length, prong spacing and wind speed. They found that the interference effects were more severe at 10 m/sec than at 40 m/sec and that these effects exhibit a steep increase for prong spacings  $< 2$  mm. and prong lengths  $< 6.5$  mm. Clearly (in hindsight) the 55A32 X-wire probe (Fig. 3) gives the worst of all worlds - four prongs instead of two, prong spacings of 0.7 mm. at best and 0.05 mm. at worst (the width of the air gap between the long prong supporting the outer end of one wire and the short prong supporting the inner end of the other wire) and prong lengths of 7 - 8 mm.

Finally, it can be seen how thermal wake interference between the wires of an X-array would cause  $v$  fluctuations to give similar polarity responses (in  $e_1$  and  $e_2$ ) to  $w$  fluctuations. (Recall from the end of section 3.2 that this conclusion was reached in order to explain the data of Table I.) Referring to the arrangement shown in Figure 4, a positive  $v$  fluctuation rotates  $U$  in a direction that tends to make wire no. 2 lie downstream of wire no. 1. The hot wake of wire no. 1 falling on wire no. 2 results in less current being supplied to wire no. 2 to maintain it at a constant temperature (and resistance). Therefore the voltage across wire No. 2 drops.

Prong and probe effects aside, this simple-minded reasoning suggests the following dynamic responses (as a first approximation) for the X-wires for positive  $v$  fluctuations:

$$\left. \begin{aligned} e_1 &= a_1 u + b_1 w, \\ e_2 &= a_2 u - b_2 w - c_2 v. \end{aligned} \right\} \quad (3-3)$$

Similarly, for negative  $v$  fluctuations, the response equations are

$$\left. \begin{aligned} e_1 &= a_1 u + b_1 w + c_1 v, \\ e_2 &= a_2 u - b_2 w. \end{aligned} \right\} \quad (3-4)$$

The constants are all positive.

### 3.5 Questions to be Answered

The experimental study of the response to  $v$  fluctuations was directed toward answering the following questions:

- (i) Is the response qualitatively like that suggested by equations (3-3) and (3-4)?
- (ii) If not, what form does the response to  $v$  take?
- (iii) How large must  $v/\bar{U}$  be before the sensitivity to  $v$  becomes important (say 10% of the sensitivity to  $u$  or  $w$ )?
- (iv) What alterations must be made to the wire mounting arrangement to ensure that the sensitivity to  $v$  is unimportant?

## CHAPTER IV. THE WIND TUNNEL EXPERIMENTS

### 4.1 Experimental Arrangement

The X-wire probe was mounted on a turntable in the 36 inch x 27 inch wind tunnel of the Dept. of Mechanical Engineering, U.B.C. The turbulence level was about 0.1%. A sketch of the arrangement is shown in Figure 5.

A block diagram of the data collection equipment is presented in Figure 6. Each wire of the X-array was heated and maintained at a constant temperature by a separate constant temperature anemometer (CTA), Disa model 55D05. The output voltage of an anemometer (i.e., the voltage  $E$  in King's Law), was then applied to a Disa Model 55D25 Auxiliary Unit. This unit was employed to perform low-pass filtering (to remove the low level of turbulence noise from the hot-wire signal) and DC suppression in order that the DC output of the anemometer would neither saturate the output of the DC amplifier nor drive the pen on the chart recorder beyond full scale.

No attempt was made to match the two wires of the X-array or to linearize the anemometer outputs since only the relative responses of the wires to  $u$ ,  $v$  and  $w$  fluctuations were of interest.

### 4.2 Experimental Procedure

Static calibrations were obtained for both wires by varying the air speed in steps and measuring the DC output of both anemometers after each step. The dynamic sensitivity to  $u$  for any operating point

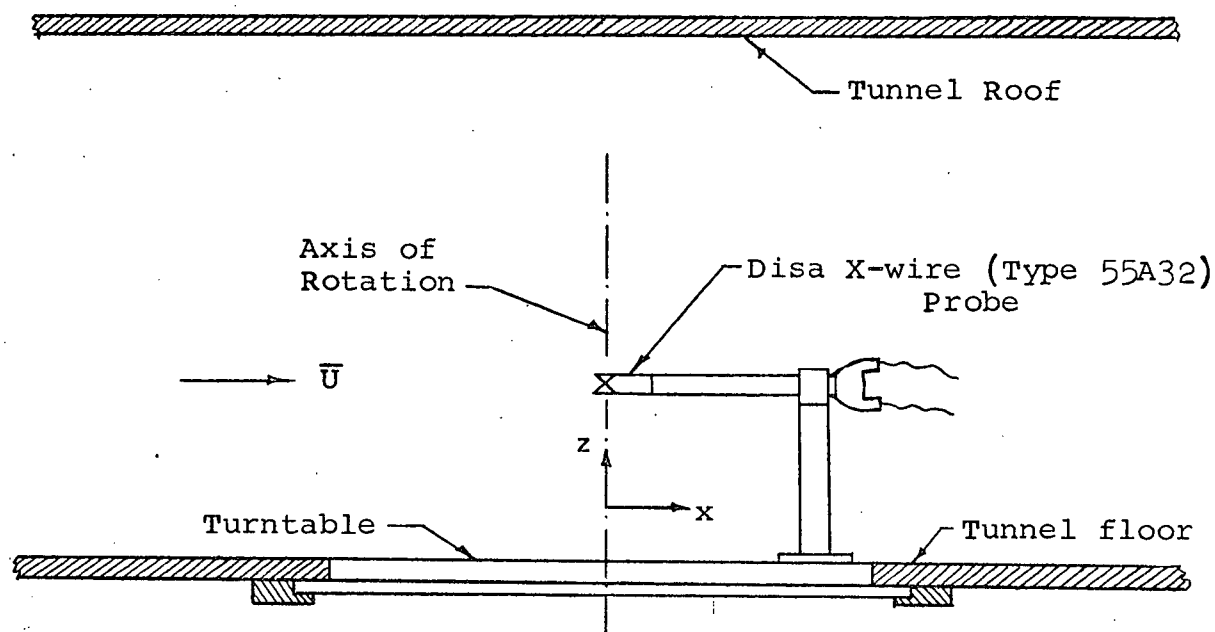
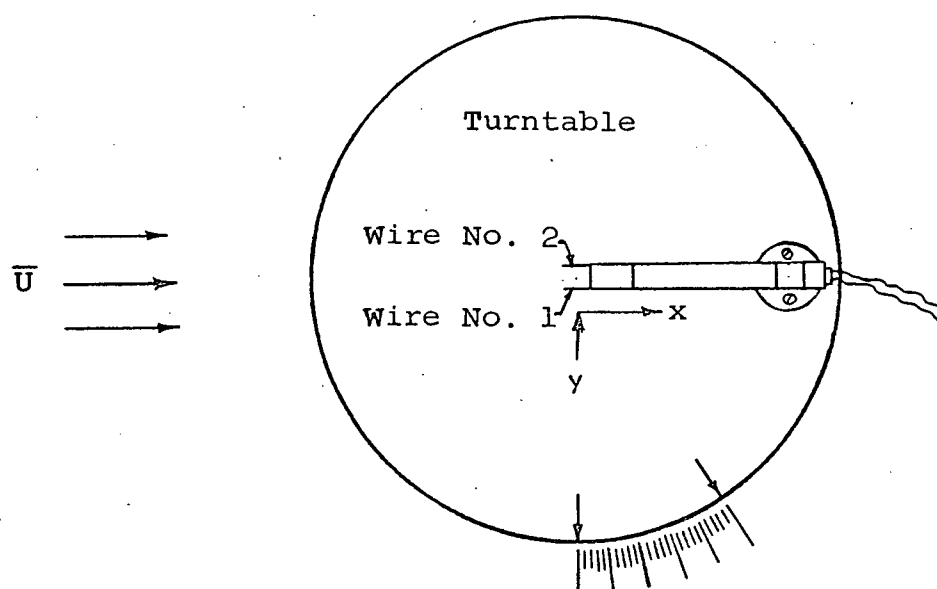
ELEVATIONPLAN VIEW

Fig. 5. Experimental Arrangement in Wind Tunnel

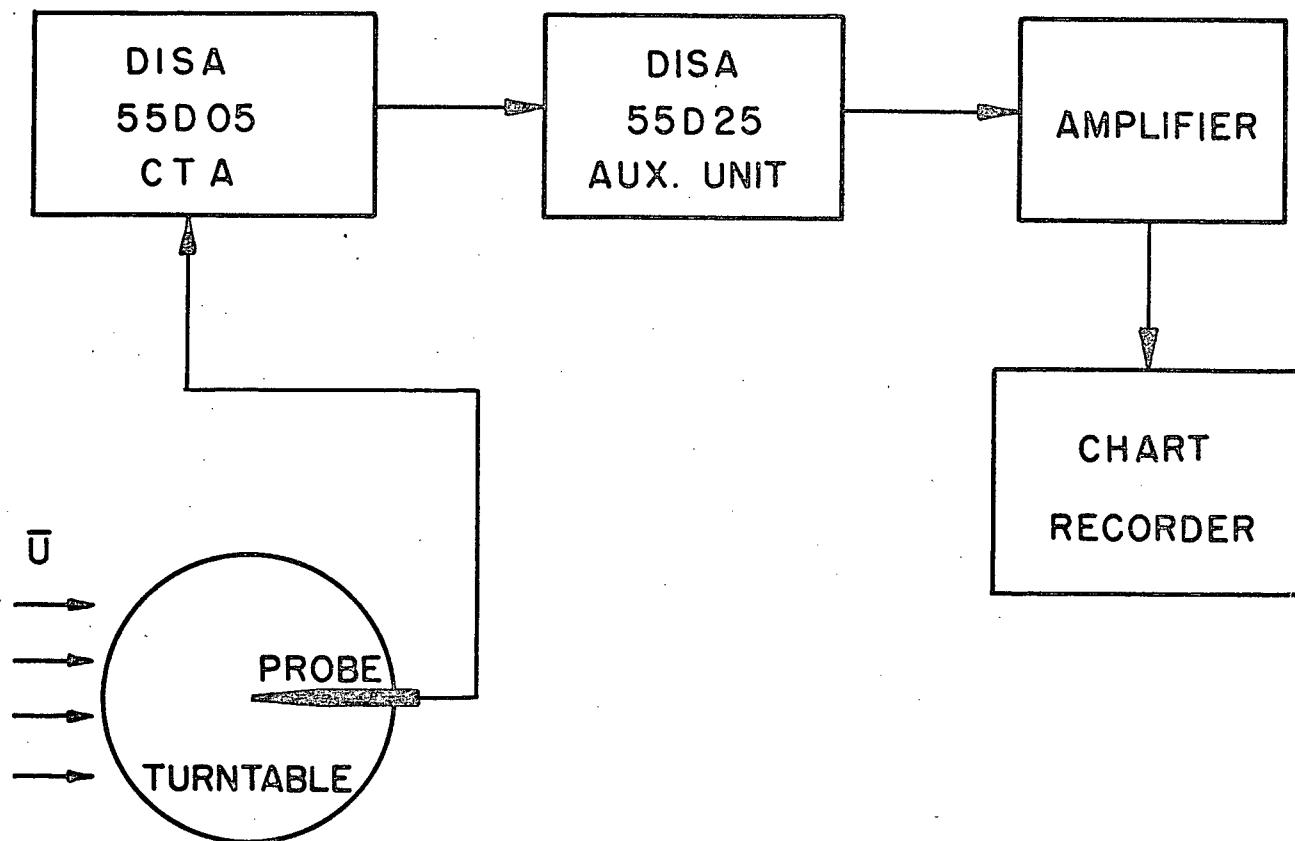


Fig. 6 Block Diagram of Equipment Used to Measure Directional Characteristics of X-Probe

$(\bar{E}, \bar{U})$  could then be calculated as described in section 2.5.

In order to determine the sensitivity of the wires to  $v$ , quasi fluctuations were introduced in the following manner. Rotating the turntable (Figure 5, lower) clockwise by an angle  $\beta$  has the same effects as leaving the turntable fixed and changing the x-component of the wind by  $\bar{U} (\cos \beta - 1)$  and the y-component by  $\bar{U} \sin \beta$ . For small  $\beta$ , the x-component "fluctuation" is considerably smaller than the y-component "fluctuation". For example,

$$(\cos \beta - 1) = 0.034 \sin \beta, \beta = 4^\circ.$$

In summary, rotating the X-array by an angle  $\beta$  is equivalent to introducing

$$v = \bar{U} \sin \beta \quad (4-1)$$

and

$$u = \bar{U}(\cos \beta - 1) . \quad (4-2)$$

Clockwise rotations must be taken as positive, counter-clockwise as negative in order that the signs of  $u$  and  $v$  are consistent with the system of axes already chosen.

"Fluctuations" of  $w$  were produced by a similar technique. First the X-array was rotated clockwise about the probe axis (as seen from behind the probe looking upwind) by  $90^\circ$ . If the coordinate system is imagined to rotate with the array then the  $xz$  plane would lie horizontally in the earth's frame of reference. Then rotating the turntable by an angle  $\gamma$  is equivalent to introducing

$$w = \bar{U} \sin \gamma \quad (4-3)$$

and

$$u = \bar{U}(\cos \gamma - 1) . \quad (4-4)$$

Again clockwise rotations must be assigned positive angles and counter-clockwise rotations negative angles.

To establish whether or not the thermal wake produces significant effects and, if so, at what value of  $v/\bar{U}$  the effects become important, the probe was rotated from  $\beta = 0$  to  $\beta = -16^\circ$  in  $2^\circ$  decrements for two cases - the "upstream" wire operating (at about  $190^\circ\text{C}$ ) and the "upstream" wire off (i.e., at ambient temperature). Note that for negative  $\beta$  and the configuration of Figure 5, wire No. 1 tends to be downstream and in the thermal wake of wire No. 2.

Then to determine the relative sensitivities of the wires to  $v$  and  $w$  fluctuations,  $\beta$ - and  $\gamma$ -rotations were respectively made in  $2^\circ$  increments from  $-10^\circ$  to  $+10^\circ$ . A mean wind speed of 4.0 m/sec was used in all experiments.

#### 4.3 Experimental Results

In converting the data from hot-wire anemometer responses to  $\beta$ - or  $\gamma$ -rotations to data on hot-wire responses to  $v$  or  $w$  fluctuations, it is necessary to correct for the introduction of

$$u = \bar{U}(\cos \beta - 1)$$

or

$$u = \bar{U}(\cos \gamma - 1)$$

upon a  $\beta$ - or  $\gamma$ -rotation respectively. The correction in the case of a  $\gamma$ -rotation will be described here.



Let  $E_1(\gamma)$  represent the voltage output of hot-wire anemometer No. 1 when the X-array has been rotated by an angle  $\gamma$ .  $E_1(0)$  represents the output for  $\gamma = 0^\circ$ . From equation (2-11),

$$E_1(\gamma) - E_1(0) = a_1 u + b_1 w .$$

Similarly the change in the output voltage of anemometer No. 2 upon a  $\gamma$ -rotation is

$$E_2(\gamma) - E_2(0) = a_2 u - b_2 w .$$

The correction terms to be subtracted from the voltage changes to eliminate the  $u$  fluctuations unavoidably introduced are  $a_1 u$  and  $a_2 u$  respectively where

$$u = \bar{U}(\cos \gamma - 1) .$$

The constants  $a_1$  and  $a_2$  are determined from equations (2-10) and (2-12).

In summary, the dynamic responses of the hot-wire anemometers to  $v$  and  $w$  fluctuations will be

$$E(\beta) - E(0) - a\bar{U}(\cos \beta - 1) \tag{4-5}$$

and

$$E(\gamma) - E(0) - a\bar{U}(\cos \gamma - 1) \tag{4-6}$$

respectively where the voltages and constants pertain to the appropriate wire of the array.

Figure 7 shows the response of the "downstream" wire to  $v$  fluctuations for the two cases of the "upstream" wire hot and cold (i.e., at ambient temperature). Note that the situation with  $\beta = 0$  and the upstream wire at the ambient temperature was chosen as the reference voltage about which deviations would be measured for both cases.

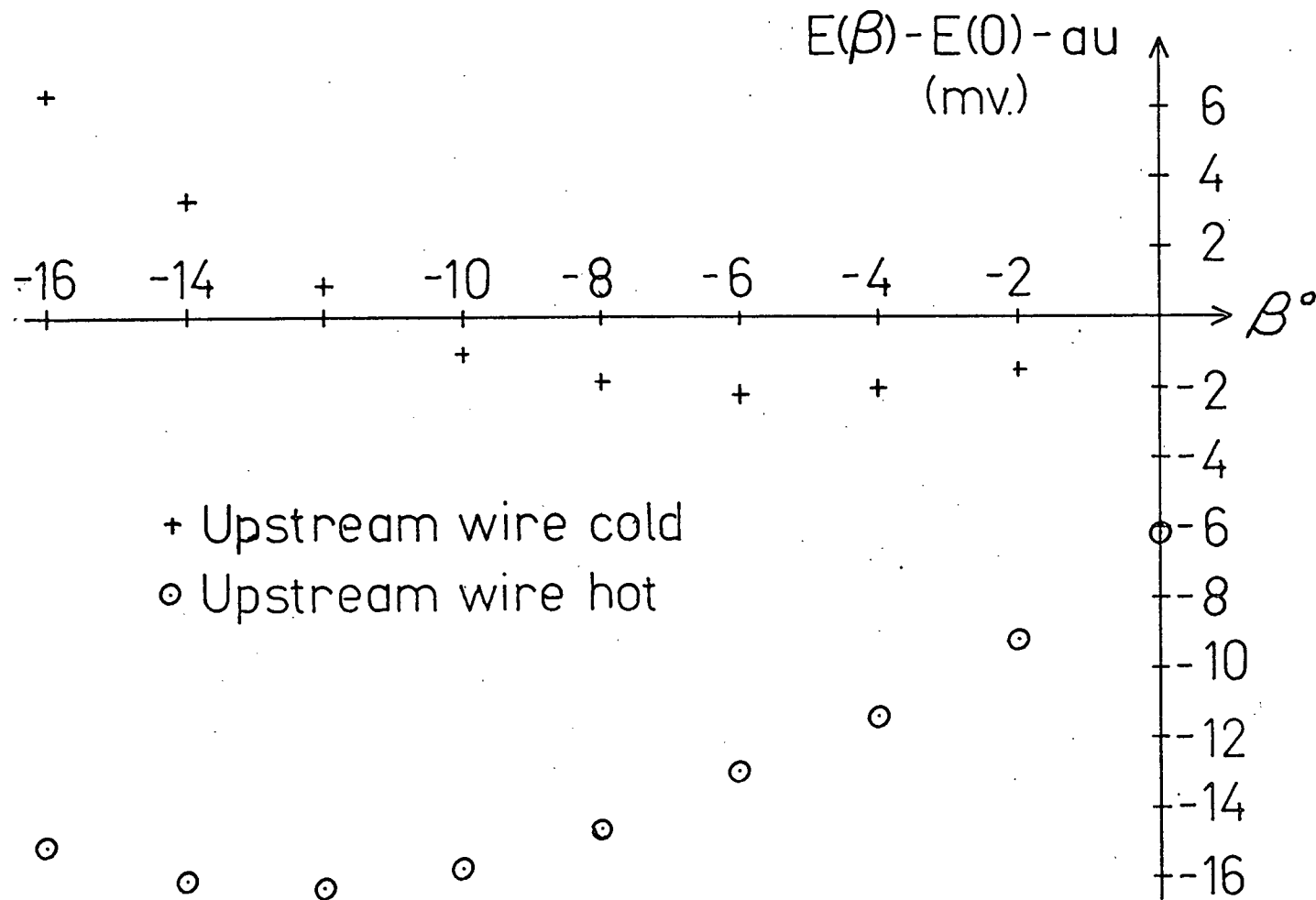


Fig. 7 v-Response of "Downstream" Wire of Disa 55A32 X-Probe

If the hot wake of the upstream wire does intercept the downstream wire, its effect is expected to be to decrease (from the "cold" wake case) the power required to maintain the downstream wire at a constant temperature. This translates into a decrease in the hot-wire current and a decrease in the voltage across the wire. That this occurs is clearly evident in Figure 7.

Two unexpected results are also indicated by Figure 7. First, even for  $\beta = 0$  i.e., neither wire tending to be downwind of the other, there was some thermal coupling between the two wires. Secondly, with the upstream wire off, the response to  $v$  fluctuations was not strictly positive. However the argument that the cooling depends on the normal component would predict an increase in the cooling rate and consequently an increase in the voltage across the inclined hot-wire as it undergoes a positive or negative  $\beta$ -rotation since either rotation "presents" a greater length of wire normal to the air flow.

Figure 8 shows the responses of the wires to  $v$  fluctuations and Figure 9 shows the responses to  $w$  fluctuations. The  $w$ -response is reasonably linear as anticipated by equations (2-11) and (2-13), although there is a small break in the slope near  $\gamma = 0$ . The  $v$ -response plots are nearly linear for positive voltage changes (when the respective wire tends to be upstream of the other wire).

#### 4.4 Discussion of Results and Conclusions

Although the thermal wake interference between the two wires of the Disa type 55A32 X-wire probe is a major factor contributing to the

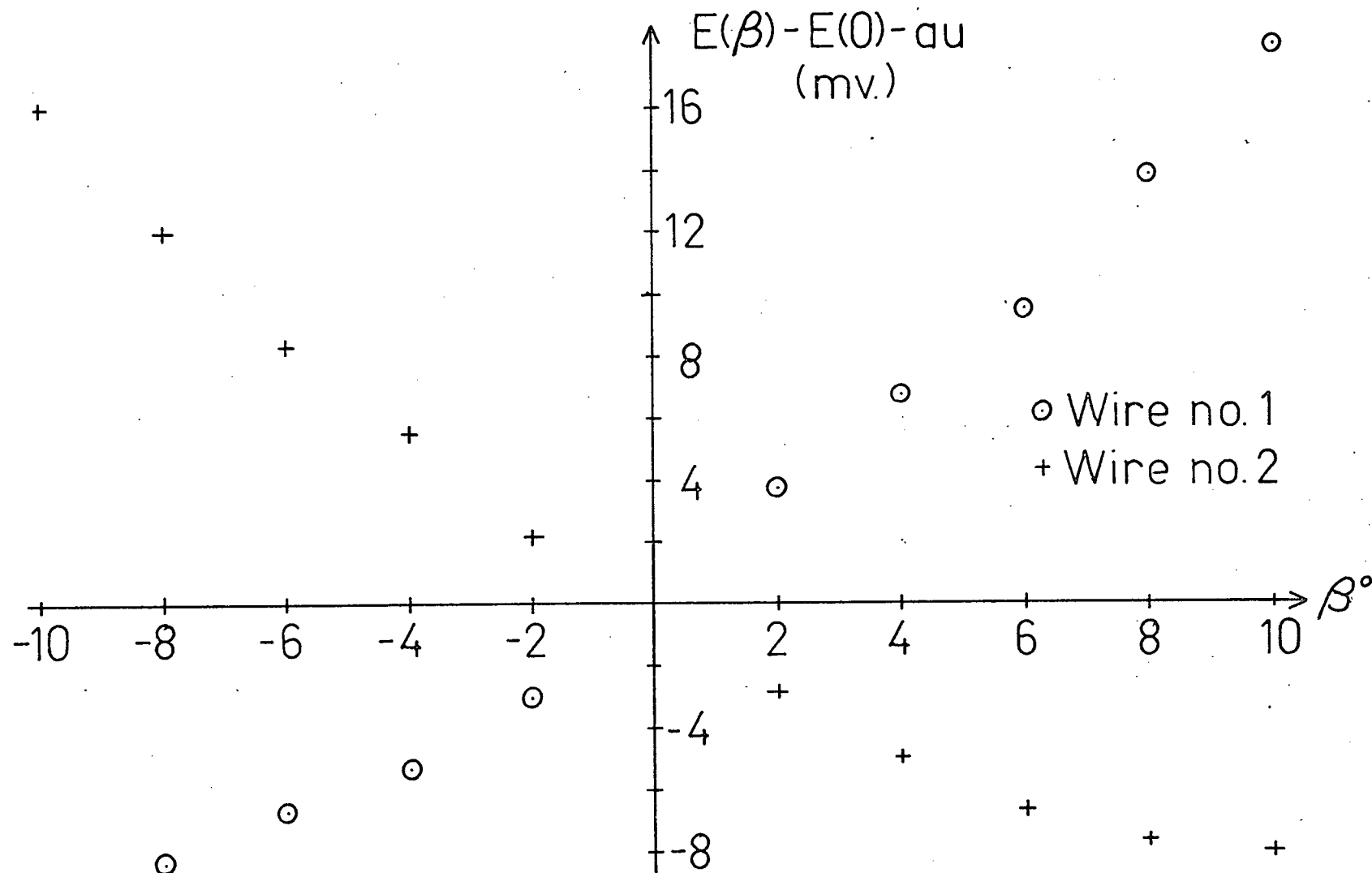


Fig. 8 v-Response of Disa 55A32 X-Probe

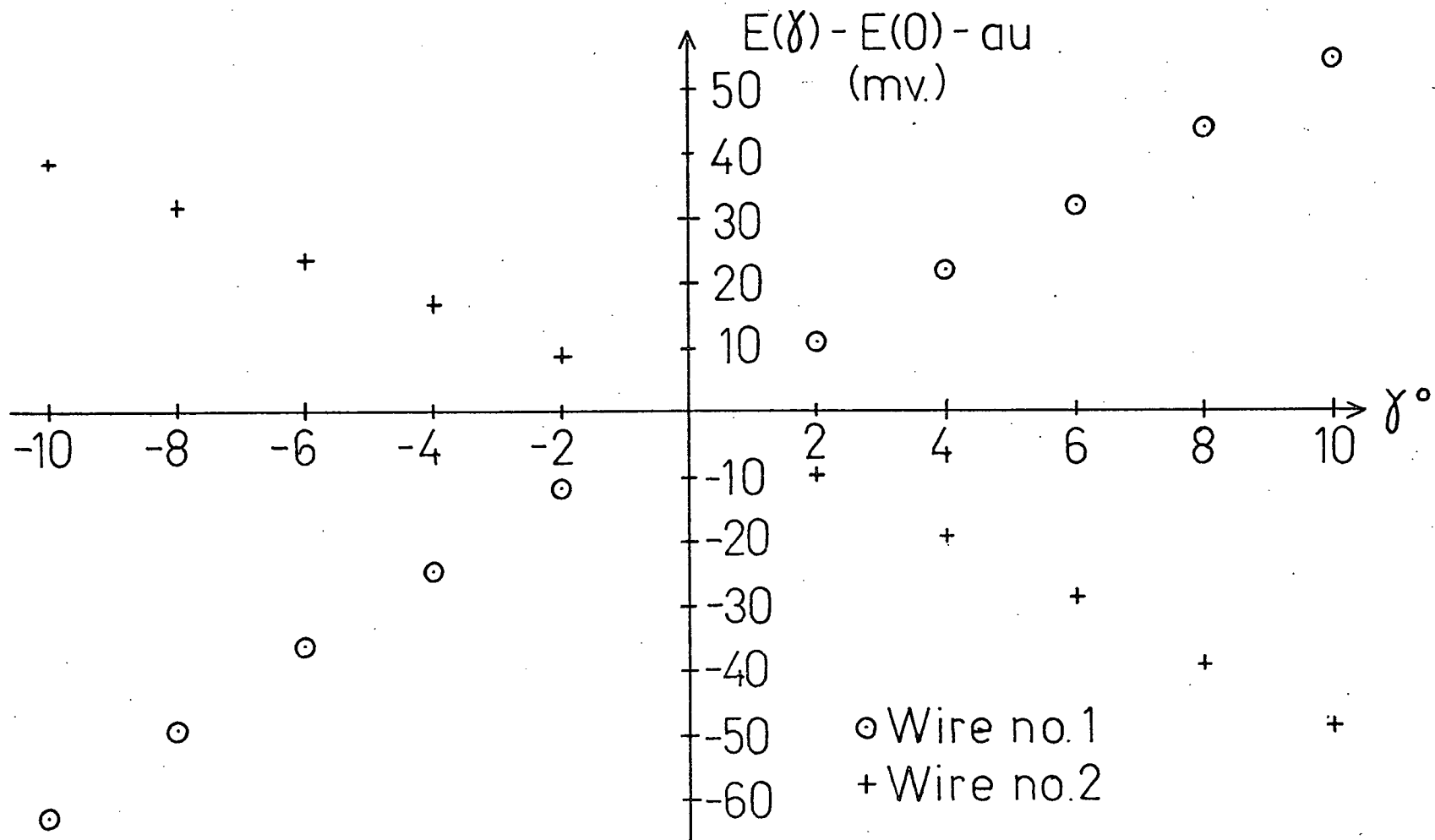


Fig. 9 w-Response of Disa 55A32 X-Probe

anomalous hot-wire results presented in Table I, there is strong evidence of other contributing factors. Figure 7 indicates that there is thermal coupling between the two wires of the array even when it is properly aligned into the wind. Data were not collected that would have enabled that graph to be extended into the region of positive  $\beta$  to determine the thermal effect of the "downstream" wire on the "upstream" wire. Such an extension would probably allow one to separate the radiative coupling from convective coupling. The former would tend to be constant (and therefore affect only the static response) while the latter should decrease for wire No. 1 with positive increase in  $\beta$ . Hinze (1959) states that radiation effects in the heat transfer to the ambient air are negligibly small under usual operating conditions of a single wire where wire temperatures do not exceed  $300^{\circ}\text{C}$ .

While the radiative coupling between the two wires remains a matter of conjecture, there is little doubt that there are some important prong and probe effects affecting the convective coupling between the wires at small  $\beta$ . (See Figure 7). Not only will the prongs broaden the hot-wire wakes in their vicinity but they will have their own thermal wakes due to the unavoidable heating of the prong tips. Champagne's data (1967) indicate that the junction of a wire and probe tip will be about  $40^{\circ}\text{C}$  above the ambient temperature.

The large sensitivity to  $v$  fluctuations relative to the sensitivity to  $w$  fluctuations must also be a prong and/or probe effect. The expected

sensitivity ratio for the experiment will be derived below assuming normal component cooling and no wake effect; this will be compared to the ratios calculated from the observed responses for both wires of the Disa 55A32 X-probe.

Consider a wire of length  $l$  inclined at  $45^0$  to  $\bar{U}$  in the wind tunnel. For a  $\beta$ -rotation, the projection of the wire's length on a plane perpendicular to  $\bar{U}$  is

$$\begin{aligned} l_{\perp} &= \{(l \sin 45^0)^2 + (l \sin 45^0 \sin \beta)^2\}^{\frac{1}{2}} \\ &= l \sin 45^0 (1 + \sin^2 \beta)^{\frac{1}{2}} . \end{aligned}$$

The response of the wire to the apparent  $v$  fluctuation corresponding to an increment  $d\beta$  in  $\beta$  will be proportional to the resulting increment,  $dl_{\perp}$ , in the component of the wire's length perpendicular to  $\bar{U}$  (according to the normal component cooling assumption). I.e.,

$$dl_{\perp} = l(1 + \sin^2 \beta)^{\frac{1}{2}} \sin 45^0 \sin \beta \cos \beta d\beta \quad (4-7)$$

Note that for  $\beta$  beginning at 0,  $dl_{\perp}$  is strictly positive.

Similarly for a  $\gamma$ -rotation and the same wind speed,

$$l_{\perp} = l \sin(45^0 + \gamma)$$

and the response to the apparent  $w$  fluctuations is proportional to

$$dl_{\perp} = l \cos(45^0 + \gamma) d\gamma . \quad (4-8)$$

Therefore, for small  $\beta$ ,  $d\beta$ ,  $\gamma$  and  $d\gamma$  and  $d\beta = d\gamma$

$$\begin{aligned} \left| \frac{v\text{-sensitivity}}{w\text{-sensitivity}} \right| &= \left| \frac{\sin \beta \cos \beta}{(1 + \sin^2 \beta)^{\frac{1}{2}}} \right| \\ &= |\sin \beta| \\ &= |\beta| . \end{aligned} \quad (4-9)$$

Note that in the positive polarity response region of Figure 8 the responses are nearly linear so that the sensitivity ratio will be nearly constant and equal to the ratio of the slope of the linear segment of the v-response to the slope of the w-response. This ratio for wire No. 1 is 0.31 and for wire No. 2 is 0.34. Equation (4-9) predicts a sensitivity ratio of 0.035 for  $\beta = 2^0$  and 0.10 for  $\beta = 5.7^0$ . Therefore the ratio for the upstream wire is qualitatively and quantitatively quite different from the expected. The v-response curve, according to the theory presented above, should be concave upwards and generally at a considerably lower magnitude over the 0 to  $10^0$  range of  $\beta$ . The excessively high response of a wire of the Disa 55A32 probe to v fluctuations which tend to put that wire in an upstream position is probably due to a combination of two factors: the flow past the wires speeding up relative to the undisplaced flow as more blockage is presented by the rotated probe and prongs and the angular-dependent convective heat loss from the prongs as proposed by Eyre (1967) and mentioned before in section 3.4.

The results of the wind tunnel testing suggest modifications that should be made to the Disa type 55A32 X-probe. The most obvious and important change is to move the two wires further apart by spreading the prongs. Although in analytical discussions of the X-wire array the wires are usually assumed to lie in the same plane, there is no real justification in attempting to duplicate the model. The smallest scale of turbulence microstructure that can be studied by a hot-wire sensor is determined by its length so that very little would be lost in the way of resolution capabilities of an X-array by separating the wires about one



wire length.

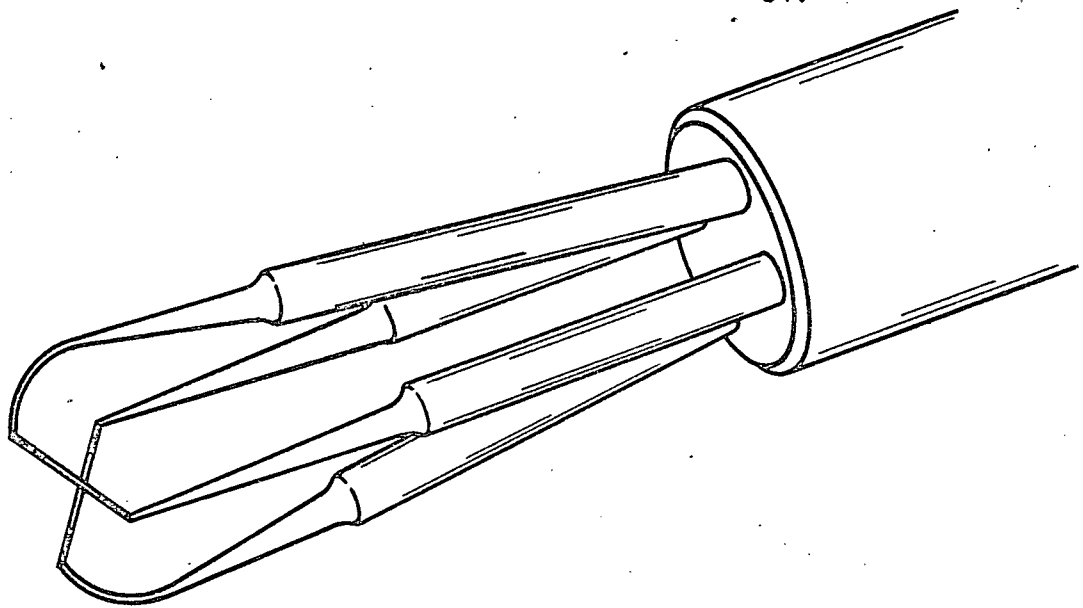
Prong effects would be reduced by the above change but they could be diminished further by lengthening the prongs - recall from section 3.4 that the findings of Dahm and Rasmussen (1969) indicated that the prong lengths used in the 55A32 probes are barely acceptable.

#### 4.5 The Thermo-Systems Model 1241 X-type Hot-Film Probe

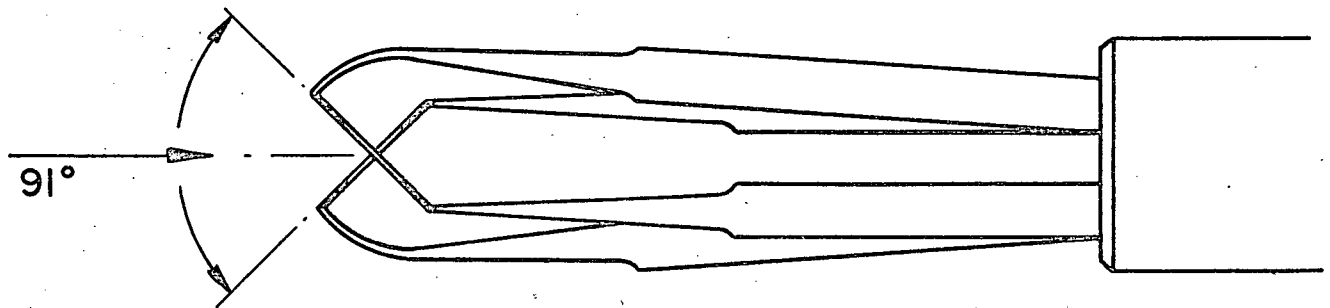
Thermo-Systems Inc. of St. Paul, Minnesota, produced an "off-the-shelf" line of X-probes which satisfied the above design criteria quite well and had two other favourable features. Their model 1241 probe with no. 20 sensor elements affixed is shown in Figure 10.

Each sensor has a 0.8 micron thick platinum film deposited by radio frequency sputtering onto a 0.002 inch diameter glass rod. The 0.040 inch sensing length, centrally located on the 0.065 inch long rod, is defined by gold plating on the ends of the rod. The gold plating also provides electrical contact with the platinum film. The rods are separated by 5/8 of the sensor length and the prongs average 11 mm. in length (compared with 7.5 mm. for the Disa 55A32 X-probe).

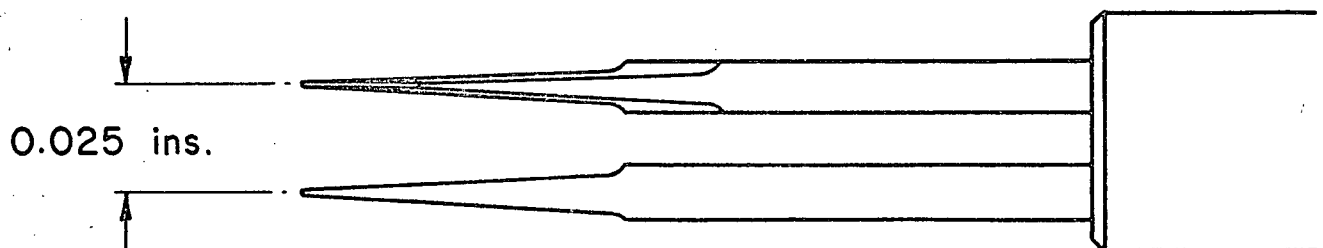
Two additional features should decrease prong effects. First, the arching structure of the two longer prongs will tend to reduce flow displacement upstream. Secondly, the hot sensing elements are not attached directly to the prongs. The gold-plated glass rod between the prong tip and the sensing segment will sharply reduce the heat conducted



VIEW OF PROBE (8 x FULL SIZE)



Quartz rod length	= 0.065 ins.
Quartz rod diameter	= 0.002 ins.
Spacing between sensors	= 0.025 ins.
Diameter of prong tip	= 0.0045 ins.
Sensing length	= 0.040 ins.



CONVENTIONAL THERMO-SYSTEMS 1241-20 PROBE  
USED IN EXPERIMENTS

Fig. 10

to the prong tip compared to the Disa 55A32 probe where the hot-wires are directly welded to the prong tips. The wakes from the prong tips should not produce any thermal effects.

Experiments were conducted with the Thermo-Systems probe to determine the response of both cylindrical hot-films to  $v$  and  $w$  fluctuations. The results are shown in Figures 11 and 12. The  $v$ -response, especially for film No. 2, is quite like that predicted by the derivation in section 4.4. It is strictly positive and concave upwards. The  $w$ -response is very nearly linear as expected. The highest ratio of  $v$ -sensitivity to  $w$ -sensitivity (the case of film No. 1 and negative  $\beta$ ) is 0.12 (compared with 0.34 for the Disa 55A32 probe). Except for film No. 1 and  $\beta$  between 0 and  $-6^\circ$ , the sensitivity ratio is equal to or smaller than that predicted by equation (4-9). The Thermo-Systems 1241-20 X-type hot-film probe appears to be free of the serious thermal wake, probe and prong interference problems that plague the Disa 55A32 X-type hot-wire probe.

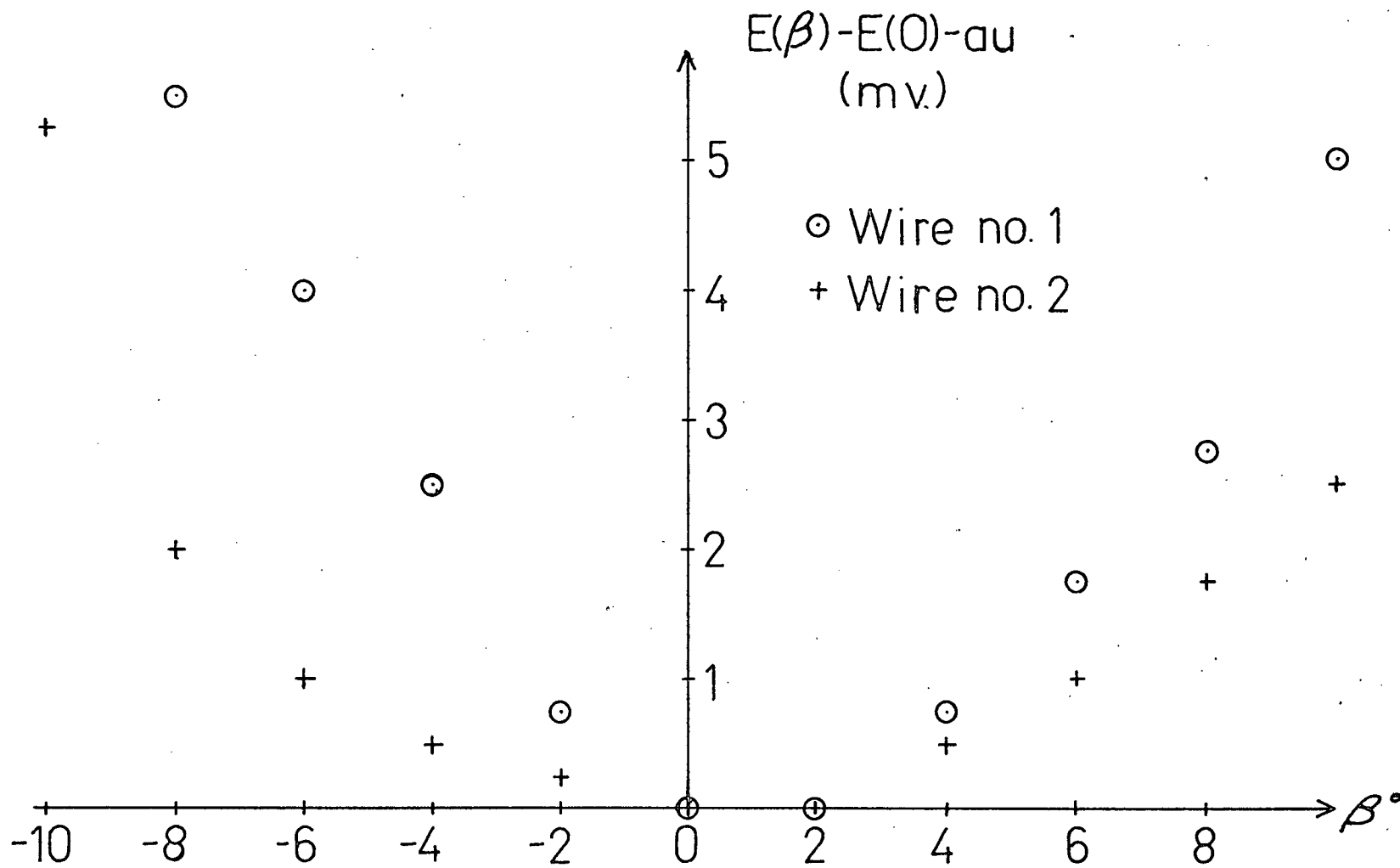


Fig. 11 v-Response of Thermo-Systems 1241-20 X-Probe

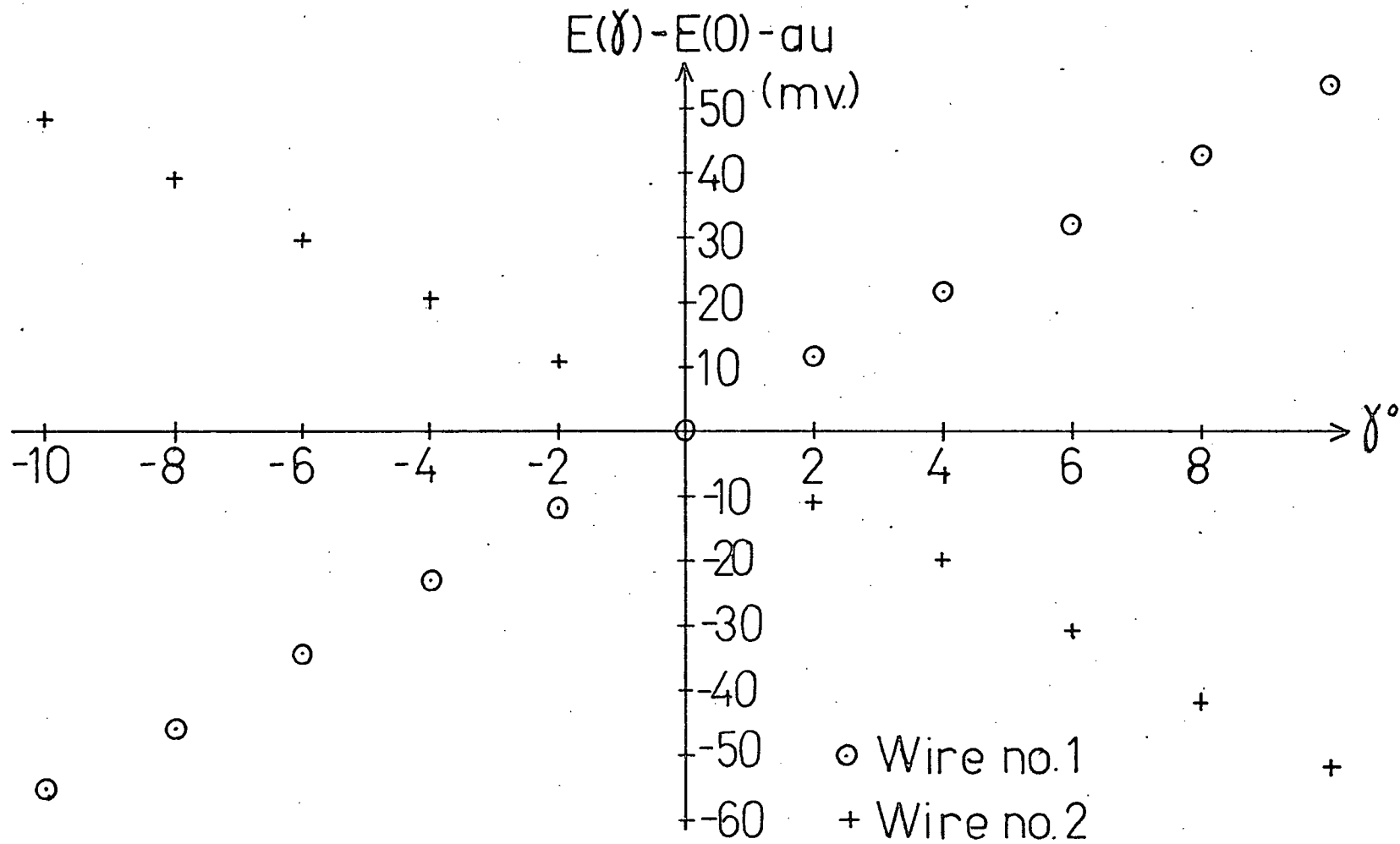


Fig. 12 w-Response of Thermo-Systems 1241-20 X-Probe

## CHAPTER V. CONSEQUENCES OF THE INTERFERENCE PROBLEMS —

5.1 On Spectral Analysis

In the analysis that led to the hot-wire spectral estimates in Table I, the hot-wires were assumed to have the instantaneous responses given by equations (2-11) and (2-13).

I.e.,

$$e_1 = a_1 u + b_1 w$$

and

$$e_2 = a_2 u - b_2 w.$$

The spectral analysis system solved this pair of simultaneous equations for  $u$  and  $w$  at every digitized data point and then computed the spectra and co-spectra as described by Garrett (1970).

In order to simplify the following derivation, assume normal component cooling with angles of inclination  $\theta_1$  and  $\theta_2$  both  $45^\circ$ . Then  $a_1 = b_1$  and  $a_2 = b_2$ . Assume further that the wire responses are identical so that  $a_1 = a_2$ . Then

$$e_1 = a_1 (u + w)$$

and

$$e_2 = a_1 (u + w) .$$

Therefore

$$u = (e_1 + e_2)/2a_1 ,$$

$$w = (e_1 - e_2)/2a_1 ,$$

$$\overline{u^2} = (\overline{e_1 + e_2})^2 / 4a_1^2, \quad (5-1)$$

$$\overline{w^2} = (\overline{e_1 - e_2})^2 / 4a_1^2 \quad (5-2)$$

and

$$\overline{uw} = (\overline{e_1 + e_2})(\overline{e_1 - e_2}) / 4a_1^2. \quad (5-3)$$

However, the wires of the Disa 55A32 X-probe have a significant response to  $v$  fluctuations. As a first approximation, this response will be taken as linear so that

$$e_1 = a_1 u + b_1 w + c_1 v$$

and

$$e_2 = a_2 u - b_2 w - c_2 v.$$

Figure 8 indicates that the response to  $v$  is very nearly linear for  $|\beta| < 40^\circ$ .

Making the same assumptions as before and taking  $c_1/b_1 = c_2/b_2 = 0.32$  - their values were observed in the experiment to be 0.31 and 0.34 in section 4.4 - the response equations become

$$e_1 = a_1 (u + w + 0.32 v)$$

and

$$e_2 = a_1 (u - w - 0.32 v).$$

In this case,

$$e_1 + e_2 = 2a_1 u$$

and

$$e_1 - e_2 = 2a_1 (w + 0.32 v)$$

so that

$$(\overline{e_1 + e_2})^2 / 4a_1^2 = \overline{u^2}, \quad (5-4)$$

$$(\overline{e_1 - e_2})^2 / 4a_1^2 = \overline{w^2} + 0.64 \overline{vw} + 0.10 \overline{v^2} \quad (5-5)$$

and

$$(\overline{e_1 + e_2})(\overline{e_1 - e_2}) / 4a_1^2 = \overline{uw} + 0.32 \overline{uv} . \quad (5-6)$$

Comparing equations (5-1), (5-2) and (5-3) with equations (5-4), (5-5) and (5-6) respectively gives (as first approximations to the sort of errors introduced by the anomalous X-wire responses)

$$\begin{aligned} \overline{u_h^2} &= \overline{u_s^2} \\ \overline{w_h^2} &= \overline{w_s^2} + 0.64 \overline{v_s w_s} + 0.10 \overline{v_s^2} \end{aligned} \quad (5-7)$$

and

$$\overline{u_h w_h} = \overline{u_s w_s} + 0.32 \overline{u_s v_s}$$

where the subscripts h and s have the same interpretation as in Table I. Because of the horizontal homogeneity (section 3.2) in the atmospheric boundary layer over the ocean,  $\overline{v_s w_s}$  and  $\overline{u_s v_s}$  are expected to be small. Therefore the major error introduced in the hot-wire spectral estimates is the  $0.10 \overline{v_s^2}$  term in  $\overline{w_h^2}$ . Note also that

$$\overline{v_s w_h} = \overline{v_s w_s} + 0.32 \overline{v_s^2} . \quad (5-8)$$

Table II shows how the measured values of  $\overline{w_h^2}$  and  $\overline{v_s w_h}$  are in much better agreement with the values calculated from the right-hand sides of equations (5-7) and (5-8) than with  $\overline{w_s^2}$  and  $\overline{v_s w_s}$  respectively. No special significance should be placed on the disagreement that still exists between the measured and calculated values because of the many assumptions that were made in deriving equations (5-7) and (5-8) and because the sensitivity ratios for the probe used in the field measurements may have been larger than 0.32.



$f \text{ (sec}^{-1}\text{)}$	$5.19 \times 10^{-2}$	$1.16 \times 10^{-1}$	$1.77 \times 10^{-1}$
$\overline{w_s^2} \text{ (m/sec)}^2$	$4.94 \times 10^{-2}$	$3.48 \times 10^{-2}$	$3.33 \times 10^{-2}$
$\overline{w_h^2} \text{ (meas.) (m/sec)}^2$	$1.41 \times 10^{-1}$	$5.34 \times 10^{-2}$	$5.19 \times 10^{-2}$
$\overline{w_h^2} \text{ (calc.) (m/sec)}^2$	$9.70 \times 10^{-2}$	$4.96 \times 10^{-2}$	$4.69 \times 10^{-2}$
$\overline{v_s w_s} \text{ (m/sec)}^2$	$6.85 \times 10^{-3}$	$5.68 \times 10^{-4}$	$5.61 \times 10^{-3}$
$\overline{v_s w_h} \text{ (meas.) (m/sec)}^2$	$2.04 \times 10^{-1}$	$6.18 \times 10^{-2}$	$5.13 \times 10^{-2}$
$\overline{v_s w_h} \text{ (calc.) (m/sec)}^2$	$1.45 \times 10^{-1}$	$4.66 \times 10^{-2}$	$3.75 \times 10^{-2}$

TABLE II: Comparison of Calculated and Measured Spectral Estimates

## 5.2 On the Results of Other Workers

Although the Disa 55A32 X-wire probe had not been used by the Institute of Oceanography at the University of British Columbia prior to the present work, it has been widely used elsewhere in the study of boundary layers, mixing regions, jets, etc. where it has been necessary to measure the downstream and one-cross stream component of the velocity fluctuation. It is clear that all measurements, regardless of whether the turbulence intensity is low or not, made with this type of probe are now suspect. In particular, measurements of shear stress and energies in the transverse component of the fluctuation in the plane of the X-array will be over-estimated.

Furthermore, many experimenters neglect to describe the probe they use and this, in the light of the present findings, becomes a meaningful omission.

## CHAPTER VI. DENOUEMENT

D.E. Guitton and R.P. Patel (Jerome, Guitton and Patel, 1971) have carried the type of research described in this thesis further to determine the dependence of the ratio of v-sensitivity to w-sensitivity of the Disa 55A32 X-wire probe on the Reynold's number of the flow. Their data are in excellent agreement with an expression they derived, i.e.,

$$\frac{\text{v-sensitivity}}{\text{w-sensitivity}} \propto \text{Re}^{-1.1} (1 + 1.31 \text{Re}^{0.4})^{-\frac{1}{2}} .$$

Translated into wind speed dependence, the ratio was about unity at 2 m/sec decreasing to about 0.1 at 20 m/sec.

As a result of problems with the Disa 55A32 X-wire probe that were demonstrated by Jerome, Guitton and Patel (1971), Disa Elektronik A/S modified their three types of X-wire probes (types 55A32, 55A38 and 55A39) by increasing the separation of the wires to 1 mm. (i.e., about one wire length). The special information note with which DISA introduced the modified probes is reproduced in the Appendix.

## BIBLIOGRAPHY

- Champagne, F. H., C. A. Sleicher and O. H. Wehrmann, 1967: Turbulence Measurements with Inclined Hot-Wires. J. Fluid Mech., 28, Part I.
- Collis, D. C. and M. J. Williams, 1959: Two-Dimensional Convection from Heated Wires at Low Reynolds Numbers. J. Fluid Mech., 6, page 357.
- Corrsin, S., 1963. Encyclopedia of Physics, Vol. VIII/2, Berlin, Springer-Verlag OHG, page 555.
- Dahm, M. and C. G. Rasmussen, 1969: Effect of Wire Mounting System on Hot-Wire Probe Characteristics. DISA Information No. 7, page 19.
- Eyre, D., 1967: End Conduction and Angle of Incidence Effects in Single Hot-Wire Anemometer Probes. IRG Report 1521 (W), United Kingdom Atomic Energy Authority.
- Garrett, J. F., 1970: Field Observations of Frequency Domain Statistics and Nonlinear Effects in Wind-Generated Ocean Waves. Ph. D. dissertation, University of British Columbia.
- Gilmore, D. C., 1967: The Probe Interference Effect of Hot-Wire Anemometers. Report No. 67-3, Mech. Eng. Res. Lab., McGill University, Montreal.
- Hinze, J. O., 1959: Turbulence. New York, McGraw-Hill, 586 pp.
- Hoole, B. J., and J. R. Calvert, 1967: The Use of a Hot-Wire Anemometer in Turbulent Flow. J. of Royal Aero. Soc., 71, page 213.
- Jerome, F. E., D. E. Guitton and R. P. Patel, 1971: Experimental Study of Thermal Wake Interference Between Closely Spaced Wires of an X-type Hot-Wire Probe. Aero. Quart., 22, page 119.
- King, L. V., 1914: On the Convection of Heat From Small Cylinders in a Stream of Fluid. Proc. Roy. Soc., (London), 214A, page 373.
- Mitsuta, Y., 1966: Sonic Anemometer-Thermometer for General Use. J. Meteor. Soc. Japan, 44, page 12.
- Norman, B., 1967: Hot-Wire Anemometer Calibration at High Subsonic Speeds. DISA Information No. 5, page 5.

- Pond, S., 1965: Turbulence Spectra in the Atmospheric Boundary Layer Over the Sea. Institute of Oceanography, University of British Columbia, Report No. 19.
- Webster, C.A.G., 1962: A Note on the Sensitivity to Yaw of a Hot-Wire Anemometer. J. Fluid Mech., 13, page 307.
- Weiler, H. S., 1966: Direct Measurements of Stress and Spectra of Turbulence in the Boundary Layer Over the Sea. Ph. D. dissertation, University of British Columbia.

APPENDIX

# DISA X-probes



## Thermal Wake Interference between the Wires of X-type Hot-wire Probes

### CTA-Note No. 14\*

Special Information

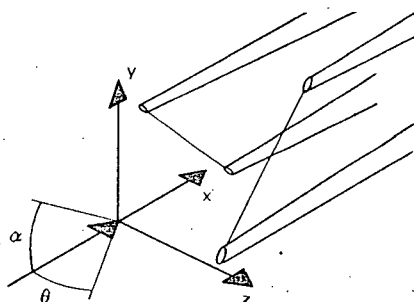


Fig. 1.

#### INTRODUCTION

X-type hot-wire probes with their two wires almost in the same plane are quite sensitive to movements of the velocity vector out of that plane. This pitching motion may cause the hot wake produced by the upstream wire to affect portions of the downstream wire, reducing the electrical power required to keep it at a constant temperature. Recent investigations of the behavior of conventional DISA X-probes, where the two wires are only 0.2 mm apart, showed these types to have very significant sensitivity to small angles of pitch at low Reynolds numbers ( $Re < 5$ ). However, this sensitivity cancels out at  $Re > 10$ .

#### THE IMPORTANCE OF PITCH SENSITIVITY IN ANALYSIS OF TURBULENCE DATA

If the pitch sensitivity is included, the response of one of the wires in an X-wire array may generally be written as

$$E = E(U, \theta, \alpha) \quad (1)$$

where  $\theta$  and  $\alpha$  are the pitch and yaw angles, respectively (see also Fig. 1).

For small changes

$$dE = \frac{\delta E}{\delta U} dU + \frac{\delta E}{\delta \alpha} d\alpha + \frac{\delta E}{\delta \theta} d\theta \quad (2)$$

or

$$e = \left( \frac{\delta E}{\delta U} \right) u + \left( \frac{1}{U} \frac{\delta E}{\delta \alpha} \right) v + \left( \frac{1}{U} \frac{\delta E}{\delta \theta} \right) w \quad (3)$$

where the bracketed terms are the sensitivity coefficients.

For convenience this relation is written as

$$e = au + bv + cw \quad (4)$$

Taking into account the sensitivity coefficients in the evaluation of  $\overline{v^2}$  from  $(e_1 - e_2)^2$ , where  $e_1$  and  $e_2$  are the instantaneous signals from the two wires, the relation between measured and actual  $\overline{v^2}$  in a two-dimensional flow is

$$\overline{v^2}_{\text{meas}} = \overline{v^2}_{\text{act}} \left( 1 + \frac{c^2}{4b^2} \frac{\overline{w^2}}{\overline{v^2}} \right) \quad (5)$$

When obtaining the shear stress  $\overline{uv}$  by taking the time averaged product of the instantaneous signals

$(e_1 + e_2)(e_1 - e_2)$  the equation between measured and actual  $\overline{uv}$  is

$$\overline{uv}_{\text{meas}} = \overline{uv}_{\text{act}} \left( 1 - \frac{c}{2a} \frac{\overline{v|w|}}{\overline{uv}} - \frac{c^2}{4ab} \frac{\overline{w|w|}}{\overline{uv}} \right) \quad (6)$$

The importance of the sensitivity to pitch can be expressed by determining the ratios  $\frac{c}{a}$  and  $\frac{c}{b}$ .

For nonlinear response

$$E^2 = A + B(U)^n \quad (7)$$

the sensitivity coefficients a and b are

$$a = \frac{1}{2E} n B(U)^{n-1} \quad (8)$$

\* This note summarizes the results of recent experiments by Jerome, Guitton, and Patel which are given in the following:

Jerome, F.E., Guitton, D. and Patel, R.P. "Experimental study of the thermal wake interference between closely spaced wires of a X-type hot wire probe (1969) (To be published.)"

Guitton, D. and Patel, R.P. "An experimental study of the thermal wake interference between closely spaced wires of a X-type hot wire probe", McGill University, M.E.R.L. Report 69-7 (1969).

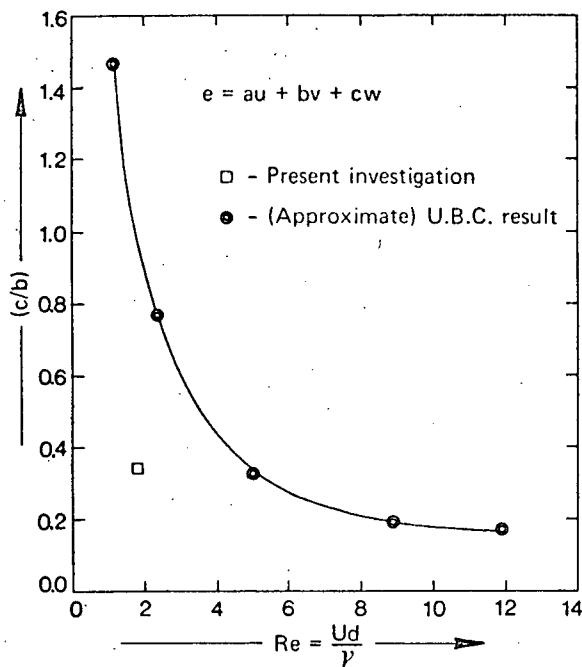


Fig. 2. Ratio of pitch to yaw sensitivity for conventional X-wires vs. Reynolds number.

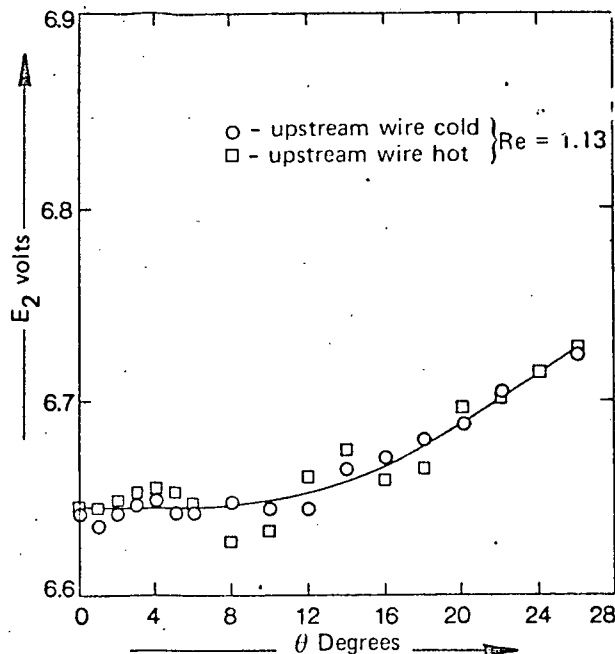


Fig. 3. Pitch response of modified X-wire probe with and without a thermal wake.

and

$$b = a \cot \alpha \quad (9)$$

if longitudinal cooling effects, which are of second order, are neglected.

The value of  $c$  is

$$c = \frac{1}{U} \frac{\delta E}{\delta \theta} \quad (10)$$

$c$ , accounting for the thermal wake interference, can be obtained by measuring the slopes of the  $\Delta E$  versus  $\theta$  plots at  $\theta = 0$ .

#### CONVENTIONAL DISA X-TYPE PROBES

Experiments carried out by Jerome, Guittou and Patel (1969) have shown that the ratio of the static pitch sensitivity to yaw sensitivity ( $c/b$ ) varies strongly with the Reynolds number. In the range of  $Re$  from 1 to 10 the ratio ( $c/b$ ) decreases from approx. 1 to 0.1 explained partly by the dependence of the yaw sensitivity  $b$  on  $Re$  and partly by the width of the thermal wake being proportional

to  $Re^{-1/2}$ . The dynamic pitch sensitivity, which might exist for measurements in a turbulent flow, appears to be similar to that taken from a static calibration.

#### NEW DISA X-TYPE PROBES

By moving the wires apart by approx. one wire length in the direction perpendicular to the plane of the X, Jerome, Guittou, and Patel observed no wake interference. On a basis of these results DISA has improved the design of its X-probes by increasing the distance between the wires to 1.0 mm instead of the present 0.2 mm.

These modifications include probe types 55A32, 55A38 and 55A39. Type numbers will not be changed. In order to distinguish between the new types with widely spaced wires and the conventional types, all new X-probes are marked with the color code, which was introduced at the end of 1969. (Conventional X-probes had type numbers engraved on the probe body.)

The color code, consisting of three dots, will be:

55A32: red - orange - red	} read from the sensor end
55A38: red - orange - grey	
55A39: red - orange - white	

# DISA

DISA ELEKTRONIK A/S . DK 2730 HERLEV . DENMARK

Telephone: Copenhagen (01) 94 52 11 . Telegrams: DISAWORKS, Copenhagen . Telex: 5849